npj | climate and atmospheric science

Article

Published in partnership with CECCR at King Abdulaziz University

https://doi.org/10.1038/s41612-024-00614-4

Climate change unevenly affects the dependence of multiple climate-related hazards in China

Xuezheng Zong [1,2], Yunhe Yin [1] ✉ & Mijia Yin [1,2]

Due to the complex natural environment and large regional differentiation in China, the dependence of multiple climate-related hazards on compound events (CEs) and their response to climate change are still unclear. Using daily meteorological observations (1961–2020) and climate simulations from the Coupled Model Intercomparison Project Phase 6, statistically strong dependences among hot, dry, and high fire risk are revealed in China. The average temperature from 1991 to 2020 was 1 °C higher than that from 1961 to 1990, and the probabilities of CEs exhibiting extreme hot-dry, dry-high fire risk, and extreme hot-dry-high fire risk increased significantly by 74.8%, 60.5%, and 26.8%, respectively. Although most CEs occur more frequently in China at the end of the 21st century, the increase rates in low emissions are lower. These findings have implications for developing climate adaptation and mitigation strategies to cope with increased CEs in critical geographical regions.

Compound events (CEs) are combinations of two or more events/hazards occurring at spatial and temporal scales, amplifying negative impacts on natural and socioecological systems compared to a single hazard[1,2]. In recent years, CEs have occurred globally, including in Australia[3,4], the Pacific Northwest[5], and China[6]. In mid-July 2022, for example, Southwest China was hit by the co-occurrence of unprecedented and long-lasting heatwaves and droughts[6], which exceeded the impacts that would have been caused by heat and dryness in isolation[7]. Recent CEs worldwide also reflect that wildfire risk easily reaches the extreme threshold under the influence of compound hot-drought events[5,8]. Extreme precipitation is another form of anomalous precipitation that can also attract attention, as it results in crop failure[9], damage to infrastructure[10], and increased insurance costs[11]. In coastal areas, extreme precipitation often coincides with strong winds or even storms[12–14] and can result in flooding[15]. Undoubtedly, these unprecedented or record-breaking events, such as heatwaves[16,17], drought[18,19], and wildfires[20,21], indicated that the occurrence, impacts, and risks of CEs have intensified in recent years, partly due to climate change.

Rising global surface and ocean temperatures drive drastic changes in climate systems, termed climate change[22]. The Coupled Model Intercomparison Project (CMIP) provides a useful tool for understanding how CEs change with climate change. There is consensus that compound drought events[23], consecutive extreme precipitation events[24], compound drought and heatwave events[25–27], compound extreme hot and extreme precipitation events[28], compound drought and wildfire events[29], and compound extreme precipitation and strong wind events[30] will become more frequent and intense across the world under high emission scenarios. Conversely, the frequency of CEs related to extreme cold events (e.g., compound cold-dry events and compound cold-wet events) will decrease in the future[28]. However, less attention has been given to the role of warming in compound event occurrence. The effects of warming on the dependence of various hazards require further investigation because rising temperature may contribute to the occurrence of other hazards[31–33]. It is well known that because of land–atmosphere feedback, heatwaves and drought often occur simultaneously and can cause compound heatwaves and drought events[31–33]. Additionally, the water-holding capacity of the atmosphere increases with rising air temperature, called the Clausius–Clapeyron (C–C) relation, leading to atmospheric instability and convection for precipitable water over a local range[34]. This leads to condensed water and sudden extreme precipitation after the end of a heatwave event[35–37]. Therefore, investigating the role of warming in the joint occurrence of multiple hazards may provide important insights into the occurrence of compound events in the future with climate change.

In this study, we hypothesize that the joint occurrence probability of various hazards has varied with climate warming over the past several decades, which may be related to hazards and compound event types. Such phenomena may continue and become more obvious under high emission scenarios in the future. To this end, we consider six hazards (namely dry, extreme hot, high fire risk, strong wind, extreme precipitation, and extreme cold) and identify 38 CEs types in China using observational data from 1961–2020[38] (Supplementary Table 1). Then we use the moving window

[1]Key Laboratory of Land Surface Pattern and Simulation, Institute of Geographic Sciences and Natural Resources Research, Chinese Academy of Sciences, Beijing 100101, China. [2]University of Chinese Academy of Sciences, Beijing 100049, China. ✉e-mail: yinyh@igsnrr.ac.cn

method to detect the changes in the joint co-occurrence of various hazards over the past six decades, and project their trends in the future based on Phase 6 of the Coupled Model Intercomparison Project.

Results

Statistical dependence among various hazards in different periods

During the first period (1961–1990), a positive dependence (LMF > 1) was detected for hazard combinations of extreme hot and dry, extreme hot and extreme precipitation, extreme precipitation and strong wind, dry and high fire risk, and high fire risk and strong wind in the study area (Fig. 1a). The LMF values between extreme hot and dry events are greater than the LMF values between the other hazard combinations. Regionally, the dependence between extreme hot and high fire risk is weak (LMF < 1) except in the northern subtropical humid region and northwest arid region. In the southern subtropical and tropical humid regions, the LMF between extreme cold and high fire risk is greater than 1 and larger than that in other eco-geographical regions during the 1961–1990 period. The dependences between extreme hot and strong wind, extreme cold and extreme precipitation, and extreme cold and dry are weaker nationwide.

A strong correlation exists between the LMF values of different hazard combinations and temperature ($|r| > 0.8$, $P < 0.01$). At the national scale, the LMF value between extreme hot and dry events increased significantly by 59.5% from the first period to the last (1991–2020) period (Fig. 1b). Notably, this increase reaches its peak in the southern subtropical and tropical humid region, registering at 95.4%. The dependence between extreme hot and extreme precipitation was also enhanced across nine eco-geographical regions with rising temperature. Compared with that in the first period, the LMF value between extreme hot and extreme precipitation events increased by 24.5% during the last period. In addition, the average LMF values between extreme precipitation and strong wind, dry and high fire risk, and high fire risk and strong wind increased to 2.2, 3.3, and 2.8, respectively, during the period of 1991–2020.

In cold temperate humid region, mid-subtropical humid region, and north semi-arid region, the dependence between extreme hot and high fire risk shifted from negative (LMF < 1) to positive (LMF > 1) during the 1991–2020, with average LMF values of 1.1, 1.6, and 1.2, respectively. This shift suggests that with rising temperatures, extreme hot and high fire risk events increasingly occur simultaneously or sequentially, leading to compound extreme hot-high fire risk events in these regions. In contrast, the dependencies between extreme cold and either extreme precipitation or dry events remained negative (LMF < 1) during the same period.

Occurrence of compound events in different periods

Nationally, a positive correlation exists between the occurrence of CEs such as extreme hot-extreme precipitation (Fig. 2a), extreme hot-dry (Fig. 2b), dry-high fire risk (Fig. 2j), and extreme hot-dry-high fire risk (Fig. 2m), and rising temperature ($r > 0.9$). During the last period (1991–2020), the average probabilities of these CEs were 0.007, 0.047, 0.036, and 0.044, respectively, marking significant increases of 21.8%, 74.8%, 60.5%, and 26.8% from the first period (1961–1990) ($P < 0.01$). Although the positive dependences (LMF > 1) between high fire risk and strong wind, extreme precipitation and strong wind indicate that they can cause compound events, the probabilities of these two CE types declined significantly in the recent three decades due to a reduction in strong wind occurrences (Supplementary Fig. 2). Additionally, the probabilities of some CEs types also show a negative correlation with temperature ($r < -0.9$), specifically for compound events related to extreme cold events (Fig. 2).

We next focus on nine eco-geographical regions and calculate the relative percentages of different compound events during the first (1961–1990) and last (1991–2020) periods (Fig. 3). The relative dominant CEs types (percentages larger than 10%) vary significantly across eco-geographical regions during the first period. In cold temperate humid region and mid-temperate humid/ subhumid region, CEs of dry-high fire risk, high fire risk-strong wind, extreme hot-dry-high fire risk, and dry-high fire risk-strong wind are the dominant types, accounting for 11–14.5% of the total (Fig. 3a, b). The above four CEs types also contribute >10% of all compound events in the warm temperate humid/sub-humid region and the north semi-arid region (Fig. 3c, d). Additionally, compound extreme cold-strong wind events constituted more than 10% of all CEs in most ecogeographical regions, except in the cold temperate humid and mid-temperate humid/ sub-humid region. The relatively dominant CEs types in the northern semiarid region also include compound extreme hot-dry events, with a percentage of 10.5% (Fig. 3g). In the north semi-arid region, compound extreme hot-dry events are also relatively dominant, accounting for 10.5% (Fig. 3d). The percentages of compound extreme hot-dry events in the southern subtropical and tropical humid region, northwest arid region, and Tibetan Plateau region are 10.5%, 12.6%, and 12%, respectively (Fig. 3f, h, i).

As temperatures rise, CEs related to hot and dry gain relative importance across nine ecogeographical regions, while the frequency of extreme

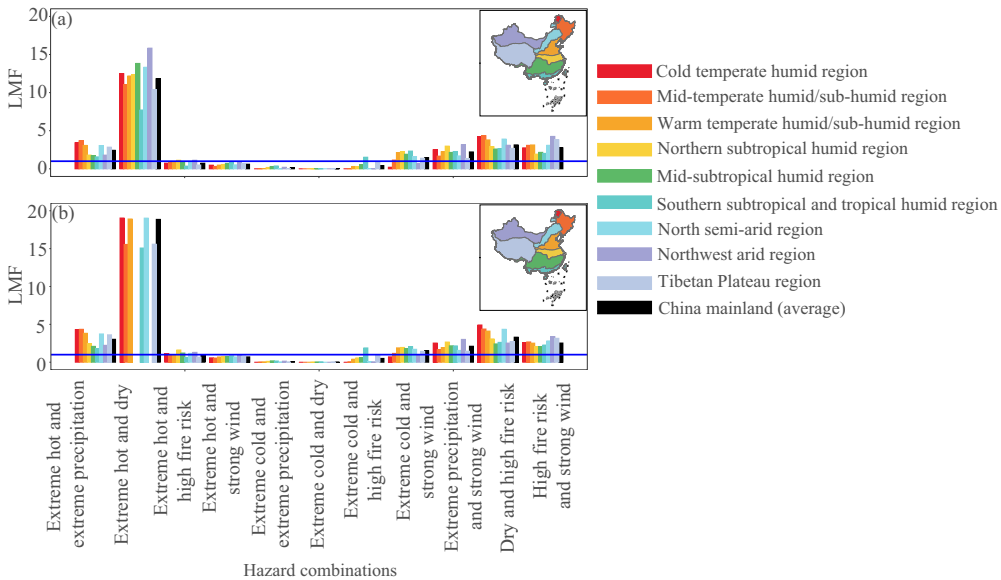

Fig. 1 | LMF plots of six hazards in different eco-geographical regions during two main periods. Where (**a**) represents the first period (1961–1990), and (**b**) indicates the last period (1991–2020). The study area was divided into nine eco-geographical regions to emphasize the features and differentiation of climate conditions.

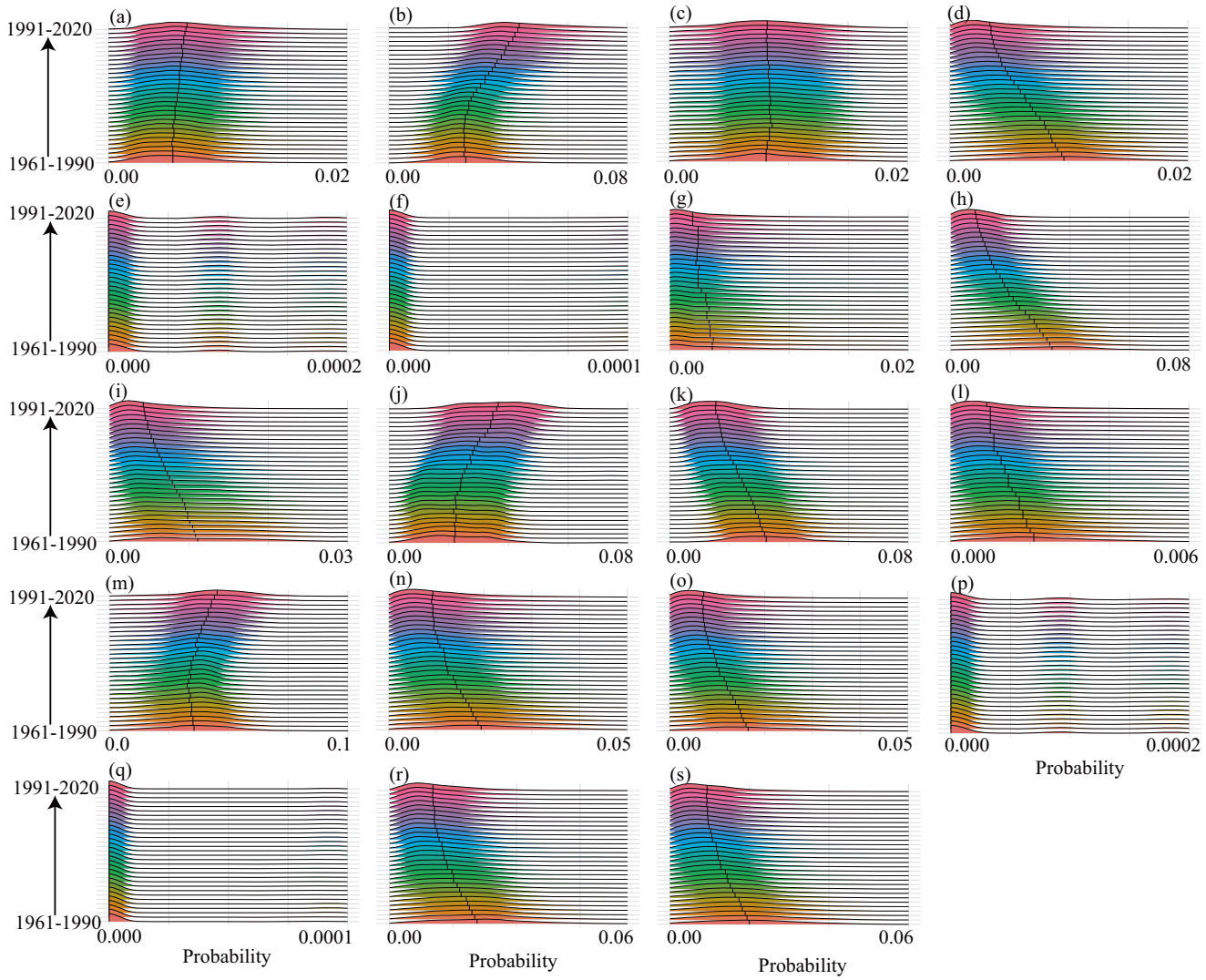

Fig. 2 | Density maps of the probability of compound events occurring during different periods. This figure represents the distribution of probabilities of various compound events in China. For a given compound event type, a higher density value means it occurred frequently and broadly in China in the study area. Where (**a**) extreme hot and extreme precipitation, (**b**) extreme hot and dry, (**c**) extreme hot and high fire risk, (**d**) extreme hot and strong wind, (**e**) extreme cold and extreme precipitation, (**f**) extreme cold and dry, (**g**) extreme cold and high fire risk, (**h**) extreme cold and strong wind, (**i**) extreme precipitation and strong wind, (**j**) dry and high fire risk, (**k**) high fire risk and strong wind, (**l**) extreme hot, extreme precipitation, and strong wind, (**m**) extreme hot, dry, and high fire risk, (**n**) extreme hot, dry, and strong wind, (**o**) extreme hot, high fire risk, and strong wind, (**p**) extreme cold, extreme precipitation, and strong wind, (**q**) extreme cold, drought, and strong wind, (**r**) dry, high fire risk, and strong wind, and (**s**) extreme hot, dry, high fire risk, and strong wind.

cold-related CEs declines. From the first to the last period, the prevalence of extreme hot-dry and extreme hot-dry-high fire risk CEs in China increased by 7.8–14.8% and 3.2–8.8%, respectively. During the last period (1991–2020), the occurrence of compound extreme hot-dry-high fire risk CEs surpassed 20% in nearly all eco-geographical regions, indicating an increased probability of wildfire from CEs.

Projection of compound events in the future

In this section, we project the occurrence and types of compound events in China under different emission scenarios (Fig. 4). Compared to the baseline (1985–2014), a significant increase in compound events related to extreme heat and dryness is anticipated, driven by the correlation between rising temperatures and low precipitation (LMF > 1), key factors in the formation of these events. Importantly, the probability of compound hot-dry events in China is projected to increase by 102.1%, 132.6%, 150%, and 156.2% in the 2030 s, under the SSP1-2.6, SSP2-4.5, SSP3-7.0, and SSP5-8.5 scenarios, respectively (Fig. 4b). These increases will exceed 200% in the 2080 s under the four scenarios. Additionally, climate change is expected to escalate the frequency of compound events involving three or four hazards, particularly CEs of extreme hot-extreme precipitation-strong wind, extreme hot-dry-high fire risk, extreme hot-dry-strong wind, dry-high fire risk-strong wind, and extreme hot-dry-high fire risk-strong wind, potentially aggravating the intensity of compound events and their impacts on important sectors in China. In contrast, the occurrence of CEs related to extreme cold events will become rare in the future, especially under high emission scenarios (SSP3-7.0 and SSP5-8.5) (Fig. 4e–g).

We further identify the dominant compound events in different eco-geographical regions in the future (Fig. 5). Climate change is expected to create uniformity in dominant CE types across different eco-geographical regions. Compound extreme hot-dry events mainly contribute to the majority of CEs in all eco-geographical regions, with percentages ranging from 43.7–85.7%. CEs related to extreme cold and strong wind are relatively less important due to their low frequency. Under the SSP5-8.5 scenario, extreme hot-dry-high fire risk and high fire risk-strong wind CEs will predominate, exceeding 15% in most regions, including cold temperate humid, northern subtropical humid, north semi-arid, northwest arid, and Tibetan Plateau regions, indicating susceptibility to wildfires. Overall, climate change is likely to reduce the variety of dominant CE types in these

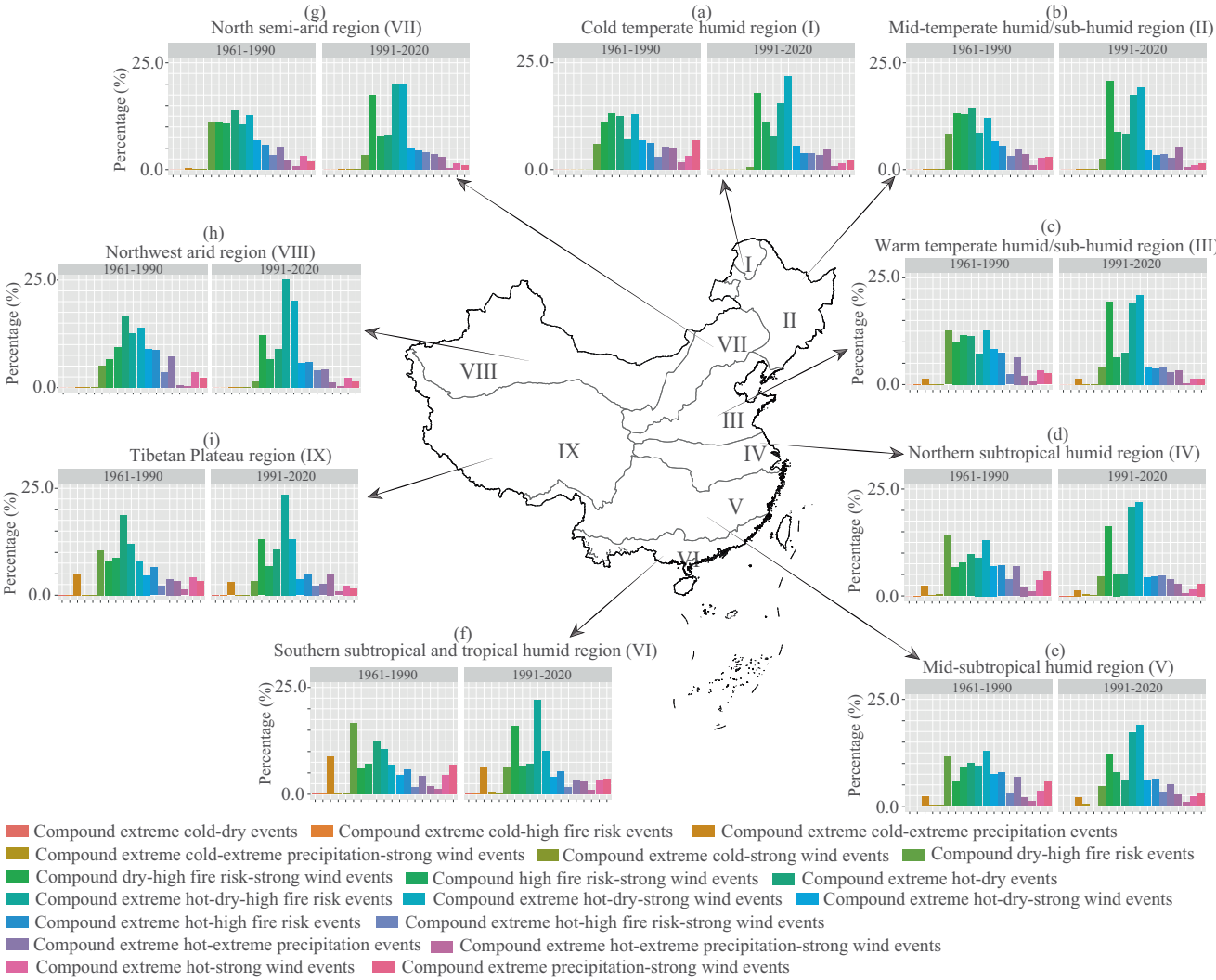

Fig. 3 | Relative percentages of compound events in different eco-geographical regions during the first (1961–1990) and last (1991–2020) periods. The percentage of each compound event type is equal to the number of occurrences divided by the number of occurrences of all compound events in the same period. Where (**a**–**i**) are the cold temperate humid region, mid-temperate humid/subhumid region, warm temperate humid/subhumid region, northern subtropical humid region, mid-subtropical humid region, southern subtropical and tropical humid region, north semi-arid region, northwest arid region, and Tibetan Plateau region, respectively.

nine eco-geographical regions in the future. The combinations of extreme hot, dry, and high fire risk are the most common in China in the future.

Discussion

Owing to climate change, the occurrence of compound events varies, as indicated by the increased probabilities of CEs related to extreme hot events[28,30,37,39] but a decreasing trend in extreme cold-related CEs (e.g., compound extreme cold-dry events)[40,41]. Recent studies have confirmed an increase in the frequency of various CE types in many regions of China, including compound extreme hot-dry events[42–44], compound extreme hot-extreme precipitation events[37,39,45], and compound extreme precipitation-strong wind events[14]. Notably, we stressed the dependence of multiple hazards on forming compound events within 1 day. We did not consider the temporal threshold when forming temporally compounding events because of the limited sample size and diverse understanding of the system[1]. While our definition sets the temporal threshold at 1 day to amplify the impacts of hazards, certain hazards may continue over a short term, forming temporally compounding events with greater negative impacts than isolated hazards. For example, one heavy rainfall event may also occur within 3 and 7 days after the end of a heat wave[37]. Thus, we recommend that the temporal threshold be determined based on the compound events database, and further analysis of interactions between multiple hazards is encouraged.

Our research identified clear evidence of climate change impacting the occurrence of CEs, likely due to dependencies among various hazards linked to land-atmosphere feedback[31–33]. Hot and dry conditions can enhance evapotranspiration but reduce fuel moisture, leading to an increase in available fuel combustion. Modeling the moisture content of fuels and potential fire behaviors, the fire weather index serves as a tool to pinpoint conditions conducive to the ignition and spread of vegetation fires[46]. Several studies have explored the correlation between fire weather and fire activities and have concluded that the frequency of extreme fire weather events and compound dry-extreme fire weather events has increased worldwide over the past decades[29,47]. Consequently, hot and dry conditions are usually precursors to mega-wildfires[48,49]. Recent extreme events worldwide also indicate that wildfire risk easily reaches the extreme threshold under the influence of compound hot-drought events[5,8]. Overall, our findings highlight the complexity of interconnected extreme events and underscore the diversity and severity of compound events in China.

Under future climate conditions, China is projected to experience increased occurrences of CEs related to extreme hot and dry events, particularly for compound extreme hot-dry events, compound dry-high fire risk events, and compound extreme hot-dry-high fire risk events. Across all eco-geographical regions, the prevalence of CEs involving extreme heat and dryness is expected to rise by the twenty-first century's end. These CEs can

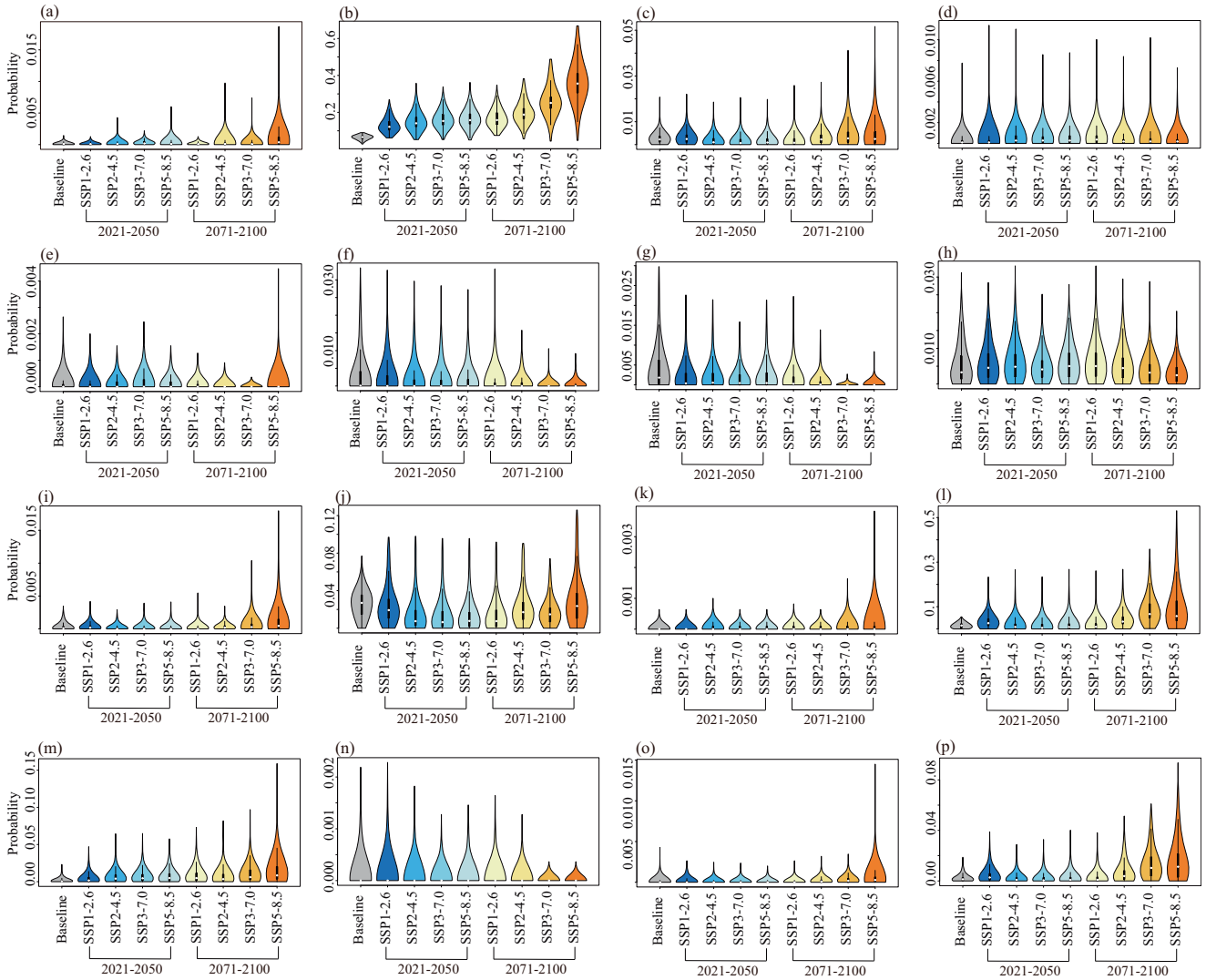

Fig. 4 | Violplots of the probability of different compound events under four scenarios in the baseline, 2030s (2021–2050 period), and 2080s (2071–2100 period). The different scale ranges were used to reflect the significant difference in the occurrence of different compound events. Larger values signify a higher probability of compound event occurrence. Where (**a**) extreme hot and extreme precipitation, (**b**) extreme hot and dry, (**c**) extreme hot and high fire risk, (**d**) extreme hot and strong wind, (**e**) extreme cold and extreme precipitation, (**f**) extreme cold and high fire risk, (**g**) extreme cold and strong wind, (**h**) extreme precipitation and strong wind, (**i**) dry and high fire risk, (**j**) high fire risk and strong wind, (**k**) extreme hot, extreme precipitation, and strong wind, (**l**) extreme hot, dry, and high fire risk, (**m**) extreme hot, dry, and strong wind, (**n**) extreme hot, high fire risk, and strong wind, (**o**) dry, high fire risk, and strong wind, (**p**) extreme hot, dry, high fire risk, and strong wind.

have significant implications for natural and artificial systems as they can lead to wildfires[50–52], crop failure, water shortages[53–55], and economic loss[56–58].

While climate change will escalate the frequency of extreme heat-related compound events, the increase is projected to be more moderate under a low emission scenario compared to high emission scenarios. Furthermore, in somes regions, the dominant CE types (exceeding 10%) under low emission futures are projected to be fewer than those under high emission scenarios. This strongly suggests that curbing emissions is crucial for mitigating future occurrences of compound events.

Methods

Extreme events and their dependence on forming compound events

The analysis uses daily meteorological observations from 2017 stations in mainland China, spanning the period from 1961 to 2020. Here, we consider a total of 6 different indices, namely daily maximum and minimum temperature, daily precipitation and wind speed, VPD (vapor pressure deficit) as a metric for meteorological dry conditions[59], and the FWI (fire weather index), calculated by the 'cffdrs' package in R software[60], to quantify fire weather conditions. An extreme event can be defined as an event that is rare at a particular place and time. Given China's diverse geographical and meteorological conditions, we use the percentile method to determine the threshold for extreme events at each station. The threshold for daily minimum temperature is set to the 10th percentile of the daily data during the historical period of each variable, while the thresholds of the other variables are set to the 90th percentile of the study period (Supplementary Table 2)[14].

As described in the previous study[38], we identify compound events (CEs) by considering the temporal sequence (simultaneous or sequential) of multiple factors (≥2) at a given station (Fig. 6). For each CEs type, the probability is calculated as the ratio of the number of days on which the event occurred to the total number of days (21,915 days of records per station) in the study period[47]. The dependence of various hazards on forming compound events is presented as the likelihood multiplication factor (LMF) (ranging from 0 to infinity)[31,47,61], which is the ratio of the actual observed probability of joint occurrence to the probability of assuming complete independence between hazard pairs. If two or more hazards are

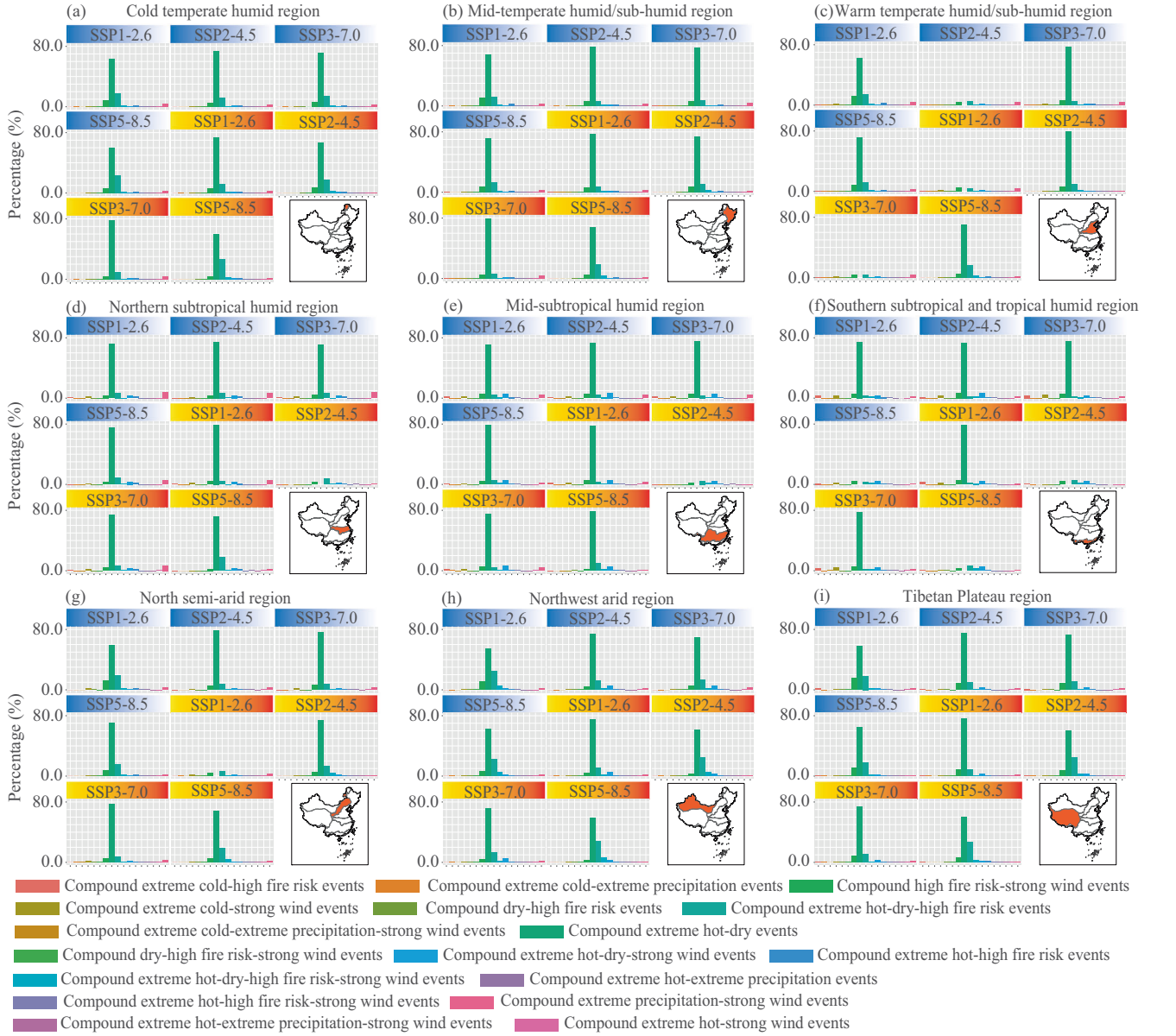

Fig. 5 | Percentages of various compound events in nine eco-geographical regions in the future under the four scenarios. The uniform rectangles filled with blue and orange represent the 2021–2050 and 2071–2100 periods, respectively. Where (**a**–**i**) are the cold temperate humid region, mid-temperate humid/sub-humid region, warm temperate humid/sub-humid region, northern subtropical humid region, mid-subtropical humid region, southern subtropical and tropical humid region, north semi-arid region, northwest arid region, and Tibetan Plateau region, respectively.

positively correlated, the LMF is greater than one; while LMF < 1 suggests a negative correlation among the occurrences of different hazards.

Selecting window size

To objectively assess the successive temporal variations in warming effects, we employ a moving window approach, avoiding artificial segmentation of the overall time series. Considering the length of the study period (1961–2020), we establish six window sizes (5–30 years) and generate run charts for daily maximum and minimum temperatures, and the mean temperature in the study area. We select a window size of 30 yr to perform subsequent analyses based on statistical significance ($R2$ and P), as this window size provided robust results while resulting in a sufficiently high number of windows as needed for the analysis (Supplementary Fig. 1). The annual average temperature in the last period (1991–2020) was 1 °C greater than that in the first period (1961–1990). For each different hazard combination, we defined it as showing a positive response to warming as its LMF significantly increased from the first moving window (1961–1990) to the last one (1991–2020) ($\alpha = 0.05$). Otherwise, we defined a negative response of compound events to warming as a significant decrease in LMF.

The CMIP6 model ensemble

The simulated climate data (1985–2100) included four climate scenarios (shared socioeconomic pathways (SSPs)1-2.6, SSP2-4.5, SSP3-7.0, and SSP5-8.5) and four general circulation modes (GCMs), CanESM5, CMCC-CM2-SR5, EC-Earth3, and EC-Earth3-Veg-LR, provided by the Inter-Sectoral Impact Model Intercomparison Project (ISI-MIP). Here, SSP1-2.6, the low end of the range of future forcing pathways (sustainability scenario), is anticipated to produce a multimodal mean of significantly less than 2 °C warming by 2100. SSP2-4.5 and SSP3-7.0 represent the medium to high ends of the range of future forcing pathways and are considered to cause radiative forcings of 4.5 and 7.0 W/m^2 by 2100, respectively. SSP5-8.5 represents the high end of the range of future pathways in which the radiative forcing levels will reach approximately 8.5 W/m^2 at the end of the 21st century[62].

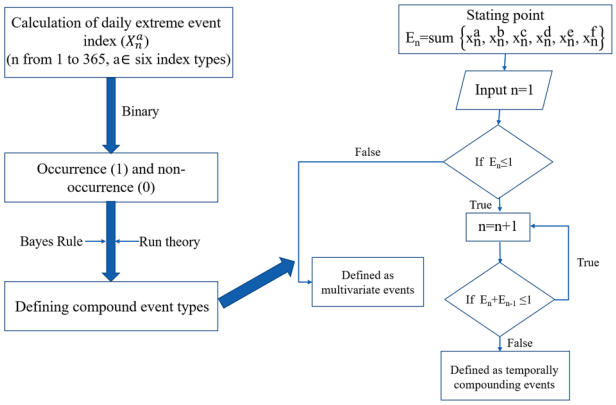

Fig. 6 | Flowchart of the definition of compound events. In the left part, the binary variable method is used to identify the occurrence of every hazard, where 1 represents the occurrence of a hazard (daily minimum temperature lower than the threshold or other five variables exceeding corresponding threshold values) and 0 represents no occurrence on a given day (i). The right part indicates how to define compound events on a daily scale. If two or more extreme events occur simultaneously or successively at a given station, it can be defined as multivariate or temporally compounding event.

To adjust the simulated data and assess the spatial variabilities in extreme event indices, the thin plate smoothing spline method was used to rasterize the daily weather data in the study area. These data were also used to correct the daily weather variables of the simulated climate data with different SSPs. Based on adjusted simulated data, we calculate six extreme event indices and identify compound events in different scenarios during the 2021–2050 and 2071–2100 periods. The baseline is set to the 1985–2014 period[63]. For each SSP scenario with four GCMs, we assumed that these models were independent and given equal weight in this study. The multimodel ensemble (MME) mean of these four GCMs was computed. This method is expected to outperform individual models in simulating global and regional climates and can provide a consensus representation of the climate system[64,65].

Data availability

The datasets generated and analyzed during the current study are not publicly available due to intellectual property and the patenting process but are available from the corresponding author for academic purposes upon reasonable request.

Code availability

Post-processing R scripts for metric computation, bootstrapping, and jitter plots are available from the corresponding author on reasonable request.

Received: 17 November 2023; Accepted: 1 March 2024;
Published online: 14 March 2024

References

1. Zscheischler, J. et al. A typology of compound weather and climate events. *Nat. Rev. Earth Env.* **1**, 333–347 (2020).
2. Seneviratne, S. I. et al. Weather and climate extreme events in a changing climate. in *Climate Change 2021: The Physical Science Basis*. Contribution of Working Group I to the Sixth Assessment Report of the Intergovernmental Panel on Climate Change 1513–1766 (Cambridge University Press, 2021).
3. Kemter, M. et al. Cascading hazards in the aftermath of Australia's 2019/2020 black summer wildfires. *Earth's Future* **9**, e2020EF001884 (2021).
4. van Oldenborgh, G. J. et al. Attribution of the Australian bushfire risk to anthropogenic climate change. *Nat. Hazards Earth Syst. Sci.* **21**, 941–960 (2021).
5. White, R. H. et al. The unprecedented Pacific Northwest heatwave of June 2021. *Nat. Commun.* **14**, 727 (2023).
6. Wang, Z., Luo, H. & Yang, S. Different mechanisms for the extremely hot central-eastern China in July–August 2022 from a Eurasian large-scale circulation perspective. *Environ. Res. Lett.* **18**, 024023 (2023).
7. Hao, Z. et al. The 2022 Sichuan-Chongqing spatio-temporally compound extremes: a bitter taste of novel hazards. *Sci. Bull.* **68**, 1337–1339 (2023).
8. Squire, D. T. et al. Likelihood of unprecedented drought and fire weather during Australia's 2019 megafires. *NPJ Clim. Atmos. Sci.* **4**, 64 (2021).
9. Lesk, C., Rowhani, P. & Ramankutty, N. Influence of extreme weather disasters on global crop production. *Nature* **529**, 84–87 (2016).
10. Dave, R., Subramanian, S. S. & Bhatia, U. Extreme precipitation induced concurrent events trigger prolonged disruptions in regional road networks. *Environ. Res. Lett.* **16**, 104050 (2021).
11. Leal, M., Boavida-Portugal, I., Fragoso, M. & Ramos, C. How much does an extreme rainfall event cost? Material damage and relationships between insurance, rainfall, land cover and urban flooding. *Hydrol. Sci. J.* **64**, 673–689 (2019).
12. Margrove, J. A. et al. Impacts of an extreme precipitation event on dipterocarp mortality and habitat filtering in a Bornean tropical rain forest. *Biotropica* **47**, 66–76 (2015).
13. Bevacqua, E. et al. Higher probability of compound flooding from precipitation and storm surge in Europe under anthropogenic climate change. *Sci. Adv.* **5**, eaaw5531 (2019).
14. Zhang, Y., Sun, X. & Chen, C. Characteristics of concurrent precipitation and wind speed extremes in China. *Weather Clim. Extrem.* **32**, 100322 (2021).
15. Stagg, C. L. et al. Extreme precipitation and flooding contribute to sudden vegetation dieback in a coastal salt marsh. *Plants* **10**, 1841 (2021).
16. Stott, P. A., Stone, D. A. & Allen, M. R. Human contribution to the European heatwave of 2003. *Nature* **432**, 610–614 (2004).
17. Mitchell, D. et al. Attributing human mortality during extreme heat waves to anthropogenic climate change. *Environ. Res. Lett.* **11**, 074006 (2016).
18. Verschuur, J., Li, S., Wolski, P. & Otto, F. E. L. Climate change as a driver of food insecurity in the 2007 Lesotho-South Africa drought. *Sci. Rep.* **11**, 3852 (2021).
19. Otto, F. E. L. et al. Anthropogenic influence on the drivers of the Western Cape drought 2015–2017. *Environ. Res. Lett.* **13**, 124010 (2018).
20. Abatzoglou, J. T. & Williams, A. P. Impact of anthropogenic climate change on wildfire across western US forests. *Proc. Natl. Acad. Sci. USA* **113**, 11770–11775 (2016).
21. Mansoor, S. et al. Elevation in wildfire frequencies with respect to the climate change. *J. Environ. Manag.* **301**, 113769 (2022).
22. Zandalinas, S. I., Fritschi, F. B. & Mittler, R. Global warming, climate change, and environmental pollution: recipe for a multifactorial stress combination disaster. *Trends Plant Sci.* **26**, 588–599 (2021).
23. Zhou, S., Zhang, Y., Park Williams, A. & Gentine, P. Projected increases in intensity, frequency, and terrestrial carbon costs of compound drought and aridity events. *Sci. Adv.* **5**, eaau5740 (2019).
24. Du, H. et al. Extreme precipitation on consecutive days occurs more often in a warming climate. *Bull. Am. Meteorol. Soc.* **103**, E1130–E1145 (2022).
25. Zhang, Q. et al. High sensitivity of compound drought and heatwave events to global warming in the future. *Earth's Future* **10**, e2022EF002833 (2022).
26. Wang, A. et al. Global cropland exposure to extreme compound drought heatwave events under future climate change. *Weather Clim. Extrem.* **40**, 100559 (2023).
27. Yin, J. et al. Global increases in lethal compound heat stress: hydrological drought hazards under climate change. *Geophys. Res. Lett.* **49**, e2022GL100880 (2022).

28. Wu, Y. et al. Global observations and CMIP6 simulations of compound extremes of monthly temperature and precipitation. *GeoHealth* **5**, e2021GH000390 (2021).
29. Richardson, D. et al. Global increase in wildfire potential from compound fire weather and drought. *NPJ Clim. Atmos. Sci.* **5**, 23 (2022).
30. Ridder, N. N., Ukkola, A. M., Pitman, A. J. & Perkins-Kirkpatrick, S. E. Increased occurrence of high impact compound events under climate change. *NPJ Clim. Atmos. Sci.* **5**, 3 (2022).
31. Zscheischler, J. & Seneviratne, S. I. Dependence of drivers affects risks associated with compound events. *Sci. Adv.* **3**, e1700263 (2017).
32. Yu, H. et al. Hotspots, co-occurrence, and shifts of compound and cascading extreme climate events in Eurasian drylands. *Environ. Int.* **169**, 107509 (2022).
33. Seneviratne, S. I. et al. Investigating soil moisture–climate interactions in a changing climate: a review. *Earth-Sci. Rev.* **99**, 125–161 (2010).
34. Berg, P., Moseley, C. & Haerter, J. O. Strong increase in convective precipitation in response to higher temperatures. *Nat. Geosci.* **6**, 181–185 (2013).
35. Molnar, P., Fatichi, S., Gaál, L., Szolgay, J. & Burlando, P. Storm type effects on super Clausius–Clapeyron scaling of intense rainstorm properties with air temperature. *Hydrol. Earth Syst. Sci.* **19**, 1753–1766 (2015).
36. Wang, G. et al. The peak structure and future changes of the relationships between extreme precipitation and temperature. *Nat. Clim. Change* **7**, 268–274 (2017).
37. You, J. & Wang, S. Higher probability of occurrence of hotter and shorter heat waves followed by heavy rainfall. *Geophys. Res. Lett.* **48**, e2021GL094831 (2021).
38. Zong, X. et al. Occurrence and hotspots of multivariate and temporally compounding events in China from 1961 to 2020. *NPJ Clim. Atmos. Sci.* **6**, 168 (2023).
39. Ning, G. et al. Rising risks of compound extreme heat-precipitation events in China. *Int. J. Climatol.* **42**, 5785–5795 (2022).
40. Wu, X., Hao, Z., Hao, F. & Zhang, X. Variations of compound precipitation and temperature extremes in China during 1961–2014. *Sci. Total Environ.* **663**, 731–737 (2019).
41. Peng, T. et al. Changes in temperature-precipitation compound extreme events in China during the past 119 years. *Earth Space Sci.* **10**, e2022EA002777 (2023).
42. Wu, X., Hao, Z., Hao, F., Singh, V. P. & Zhang, X. Dry-hot magnitude index: a joint indicator for compound event analysis. *Environ. Res. Lett.* **14**, 064017 (2019).
43. Zhang, Y., Hao, Z., Feng, S., Zhang, X. & Hao, F. Comparisons of changes in compound dry and hot events in China based on different drought indicators. *Int. J. Climatol.* **42**, 8133–8145 (2022).
44. Yu, R. & Zhai, P. More frequent and widespread persistent compound drought and heat event observed in China. *Sci. Rep.* **10**, 14576 (2020).
45. Wu, S. et al. Increasing compound heat and precipitation extremes elevated by urbanization in South China. *Front. Earth Sc-Switz.* **9**, 636777 (2021).
46. Field, R. D. et al. Development of a global fire weather database. *Nat. Hazards Earth Syst. Sci.* **15**, 1407–1423 (2015).
47. Ridder, N. N. et al. Global hotspots for the occurrence of compound events. *Nat. Commun.* **11**, 5956 (2020).
48. Wang, X., Swystun, T., Oliver, J. & Flannigan, M. D. One extreme fire weather event determines the extent and frequency of wildland fires. *Environ. Res. Lett.* **16**, 114031 (2021).
49. Thompson, D. K., Simpson, B. N., Whitman, E., Barber, Q. E. & Parisien, M.-A. Peatland hydrological dynamics as a driver of landscape connectivity and fire activity in the boreal plain of Canada. *Forests* **10**, 534 (2019).
50. Zong, X., Tian, X., Yao, Q. & Brown, P. M. An analysis of fatalities from forest fires in China, 1951–2018. *Int. J. Wildland Fire* **31**, 507–517 (2022).
51. Tang, X., Machimura, T., Li, J., Yu, H. & Liu, W. Evaluating seasonal wildfire susceptibility and wildfire threats to local ecosystems in the largest forested area of China. *Earth's Future* **10**, e2021EF002199 (2022).
52. Robinne, F.-N. et al. A global index for mapping the exposure of water resources to wildfire. *Forests* **7**, 22 (2016).
53. Su, B. et al. Drought losses in China might double between the 1.5 °C and 2.0 °C warming. *Proc. Natl. Acad. Sci. USA* **115**, 10600–10605 (2018).
54. Jia, H. et al. High emissions could increase the future risk of maize drought in China by 60–70%. *Sci. Total Environ.* **852**, 158474 (2022).
55. Yu, C. et al. Assessing the impacts of extreme agricultural droughts in China under climate and socioeconomic changes. *Earth's Future* **6**, 689–703 (2018).
56. Yang, J., Huo, Z., Li, X., Wang, P. & Wu, D. Hot weather event-based characteristics of double-early rice heat risk: a study of Jiangxi province, South China. *Ecol. Indic.* **113**, 106148 (2020).
57. Sun, Q., Miao, C., AghaKouchak, A. & Duan, Q. Unraveling anthropogenic influence on the changing risk of heat waves in China. *Geophys. Res. Lett.* **44**, 5078–5085 (2017).
58. Xia, Y. et al. Assessment of the economic impacts of heat waves: a case study of Nanjing, China. *J. Clean. Prod.* **171**, 811–819 (2018).
59. Williams, A. P. et al. Observed impacts of anthropogenic climate change on wildfire in California. *Earth's Future* **7**, 892–910 (2019).
60. Wang, X. et al. cffdrs: an R package for the Canadian forest fire danger rating system. *Ecol. Process* **6**, 5 (2017).
61. Zhou, S. et al. Land–atmosphere feedbacks exacerbate concurrent soil drought and atmospheric aridity. *Proc. Natl. Acad. Sci. USA* **116**, 18848–18853 (2019).
62. O'Neill, B. C. et al. The scenario model intercomparison project (ScenarioMIP) for CMIP6. *Geosci. Model Dev.* **9**, 3461–3482 (2016).
63. Cook, B. I. et al. Twenty-first century drought projections in the CMIP6 forcing scenarios. *Earth's Future* **8**, e2019EF001461 (2020).
64. Tebaldi, C. & Knutti, R. The use of the multi-model ensemble in probabilistic climate projections. *Philos. Trans. A Math. Phys. Eng. Sci.* **365**, 2053–2075 (2007).
65. Semenov, M. A. & Stratonovitch, P. Use of multi-model ensembles from global climate models for assessment of climate change impacts. *Clim. Res.* **41**, 1–14 (2010).

Acknowledgements

This study received financial support from National Natural Science Foundation of China (42377460) and the Second Tibetan Plateau Scientific Expedition and Research Program (2019QZKK0403) supported this study.

Author contributions

Xuezheng Zong: conceptualization, methodology, investigation, writing—original draft and revised. Yunhe Yin: conceptualization, methodology, investigation, resources, supervision, writing—review. Mijia Yin: methodology, investigation, writing—revised.

Competing interests

The authors declare no competing interests.

Additional information

Supplementary information The online version contains supplementary material available at https://doi.org/10.1038/s41612-024-00614-4.

Correspondence and requests for materials should be addressed to Yunhe Yin.